Cell and Tissue Research (2019) 376:71–81
https://doi.org/10.1007/s00441-018-2972-1

REGULAR ARTICLE

Long-chain fatty acid-induced intracellular signaling in GPR120-expressing brush cells at the limiting ridge of the murine stomach

Patricia Widmayer[1] · Lisa Hischer[1] · Katja Hennemann[1] · Soumya Kusumakshi[2] · Ulrich Boehm[2] · Heinz Breer[1]

Received: 12 July 2018 / Accepted: 23 November 2018 / Published online: 17 December 2018
© Springer-Verlag GmbH Germany, part of Springer Nature 2018

Abstract

Brush cells at the gastric groove have been proposed to operate as sensory cells capable of sensing constituents of ingested food. Recent studies have indicated that these cells express GPR120 (also known as FFAR4), the G protein-coupled receptor for long-chain fatty acids (LCFAs). However, functional implications of this receptor in brush cells have remained elusive. Here, we show that a great proportion of brush cells express GPR120. We used phosphorylation of the extracellular signal-regulated kinases 1/2 (ERK1/2) as a readout to monitor brush cell responses to the LCFAs oleic acid and α-linolenic acid. Our results demonstrate that ERK1/2 phosphorylation is increased upon exposure to both fatty acids. Increased ERK1/2 phosphorylation is accompanied by upregulated mRNA and protein levels of cyclooxygenase 2 (COX-2), a key enzyme for prostaglandin biosynthesis. Immunohistochemical experiments confirmed that oleic acid caused ERK1/2 phosphorylation and induced COX-2 expression in brush cells. Our results indicate that LCFA sensing elicits a signaling process in brush cells that may be relevant for a local regulation of gastric functions.

Keywords Brush cell · Gastric groove · GPR120 · Fatty acid sensing · COX-2

Abbreviations

ALA	α-Linolenic acid
COX-1	Cyclooxygenase 1
COX-2	Cyclooxygenase 2
DAPI	4′,6-Diamidino-2-phenylindole
DIC	Differential interference contrast
ERK1/2	Extracellular signal-regulated kinases 1/2
FA	Fatty acids
FFAR	Free fatty acid receptor
GPCR	G protein-coupled receptor
LCFA	Long-chain fatty acid
PLCβ2	Phospholipase C β2
TRPM	Transient receptor potential cation channel, subfamily M, member 5

✉ Patricia Widmayer
widmayer@uni-hohenheim.de

[1] Institute of Physiology, University of Hohenheim, Garbenstrasse 30, 70599 Stuttgart, Germany

[2] Experimental Pharmacology, Center for Molecular Signaling (PZMS), Saarland University School of Medicine, Homburg, Germany

Introduction

The stomach of rodents is divided into two well-defined compartments, the non-glandular fundus, which serves as a reservoir for food and the glandular corpus, where the actual digestive processes take place (Frantz et al. 1991; Matsukura and Asano 1997). Precisely at the transition zone from the non-glandular reservoir compartment to the glandular digestive compartment, anatomically defined as the limiting ridge, clusters of brush cells, also known as tuft, caveolated, multivesicular, or fibrillovesicular cells, are arranged in a palisade-like manner forming a band, which borders the whole length of the corpus epithelium (Luciano and Reale 1992). Based on the observation that typical gustatory signal transduction elements, such as gustducin, phospholipase C β2 (PLCβ2) and transient receptor potential cation channel, subfamily M, member 5 (TRPM5) are all expressed in these cells (Höfer et al. 1996; Hass et al. 2007; Eberle

et al. 2013a, b), it has been proposed that they may be capable of sensing constituents of the ingested food. In search for possible functions of brush cells at this strategic location, previous experiments provided some evidence that these cells express the G protein-coupled receptor (GPCR) GPR120 (also known as free fatty acid receptor 4, FFAR4) (Janssen et al. 2012) for long-chain fatty acids (LCFAs) (> C12) (Hirasawa et al. 2005; Tanaka et al. 2008). However, the functional role of this fatty acid receptor in brush cells has remained elusive.

GPR120 has been reported to interact with downstream signaling molecules, such as the extracellular signal-regulated kinases 1/2 (ERK1/2) (Brown and Sacks 2009), in different cell types. GPR120-induced ERK1/2 phosphorylation has been shown to be linked to the activation of the prostaglandin endoperoxide synthase 2, also called cyclooxygenase 2 (COX-2), which in turn causes prostaglandin release (Liu et al. 2014). Based on the observation that brush cells express the rate-limiting enzymes for prostaglandin biosynthesis of COX-1 and COX-2 and the hypothesis that they may use prostaglandins for paracrine signaling (Kugler et al. 1994; Eberle et al. 2013b; Schütz et al. 2015), we analyzed whether ERK1/2 phosphorylation and COX-2 expression might be induced by fatty acids through GPR120. To do this, we used the GPR120 ligands oleic acid and α-linolenic acid (ALA) as stimuli and monitored ERK1/2 phosphorylation as a readout for fatty acid-induced responses. Subsequently, we analyzed COX-2 as a possible downstream target of GPR120 activation. Our results provide the first evidence that oleic acid and ALA elicit signaling events in brush cells that lead to ERK1/2 phosphorylation and an induction of COX-2 expression.

Materials and methods

Mice

Studies were performed with male C57/BL6J and TRPM5-IRES-Cre/eR26-τGFP (Kusumakshi et al. 2015) mice at the age of 3 months. Mice were housed with a 12-h light/dark cycle in groups at the Central Unit for Animal Research at the University of Hohenheim and had access to standard laboratory chow and water ad libitum. Experiments were carried out in accordance with the Council Directive 2010/63EU of the European Parliament and the Council of 22 September 2010 on the protection of animals used for scientific purposes. The work was approved by the Committee on the Ethics of Animal Experiments at the Regierungspräsidium Stuttgart (V318/14 PHY) and the University of Hohenheim Animal Welfare Officer (T125/14 PHY, T126/14 PHY).

Tissue preparation

For tissue preparations, animals were killed by cervical dislocation and subsequent decapitation. The storage compartment fundus was removed, the stomach opened along the greater curvature and the ingesta either washed off with phosphate-buffered saline (PBS, 0.85% NaCl, 1.4 mM KH_2PO_4, 8 mM Na_2HPO_4, pH 7.4) for immunohistochemical analyses or with buffer solution (120 mM NaCl, 5 mM KCl, 1.6 mM K_2HPO, 25 mM $NaHCO_3$, pH 7.4) for real-time qPCR and Western blotting.

For immunohistochemical studies, a preparation technique was used as previously described (Eberle et al. 2013a). The dissected stomach was immersion-fixed in 4% paraformaldehyde in PBS for either 2 h (for COX-2, pERK1/2, ERK1/2) or 48 h (for GPR120) at 4 °C followed by cryoprotection in 25% sucrose at 4 °C overnight. The tissue was then placed in Tissue Freezing Medium and quickly frozen on liquid nitrogen. Cryosections (6–8 μm) were generated using a CM3050S cryostat (Leica Microsystems, Bensheim, Germany) and mounted on Superfrost Plus microscope slides (MenzelGläser, Braunschweig, Germany).

For qPCR and Western blot analyses, narrow strips comprising the brush cell–containing surface epithelium were excised from the opened cleaned stomach that was pinned flat with the mucosa facing up. These strips included traces of the uppermost glandular layer of the corpus and remnants of the limiting ridge.

For the purposes of stimulus application, the stomach was divided into equal halves by further separating the stomach along the lesser curvature. One half served as the control and the other was used for the stimulation. Then, either brush cell–containing strips (qPCR) or stomach halves (Western blot) were placed in 37 °C prewarmed buffer solution for 30 min. This preincubation was followed by an exposure to either buffer solution or to 10 mM oleic acid (Sigma Aldrich, Schnelldorf, Germany) or 10 mM α-linolenic acid (Sigma Aldrich) for 5 min (analysis of COX-2 mRNA levels and ERK1/2, pERK1/2 protein levels) or 10 min (analysis of COX-2 protein levels). Following exposure, strips were excised and Western blot analyses performed. Additionally, strips containing only the limiting ridge were isolated and served as controls. All samples were immediately transferred into a collection tube and frozen in liquid nitrogen.

Immunohistochemistry

Cryosections were air-dried, rinsed in PBS for 10 min and incubated with blocking solution (PBS with 10% normal donkey serum (NDS), 0.3% Triton X-100) for 60 min at room temperature. After washing in PBS three times, sections were treated with either rabbit anti-GPR120 (1:100; SAB4501490, Sigma Aldrich, Steinheim, Germany), rabbit anti-ERK1/2

(1:200; #9102, Cell Signaling Technology, Frankfurt, Germany), rabbit anti-pERK1/2 (1:100; #4370, Cell Signaling Technology), chicken anti-GFP (1:400; ab13970, Abcam, Cambridge, UK), rabbit anti-TRPM5 (1:400; serum directed against the C-terminal peptide ARDREYLESGLPPSDT, courtesy of T. Gudermann and V. Chubanov), mouse anti-acetylated-α-tubulin antibody (1:100; T6199, Sigma Aldrich), or goat anti-COX-2 (1:200; sc-1747, Santa Cruz Biotechnology) antisera, all diluted in PBS containing 10% NDS and 0.3% Triton X-100 at 4 °C overnight. Specificity and use of the antibodies were documented elsewhere (GPR120, Widmayer et al. 2015; pERK1/2, Symonds et al. 2015; GFP, van der Heijden et al. 2016; TRPM5, Kaske et al. 2007; COX-2, Schütz et al. 2015; acTub, Saqui-Salces et al. 2011). On the next day, the slides were washed three times in PBS. Primary antibodies were visualized using appropriate secondary antibodies conjugated to Alexa 488 (Dianova, Hamburg, Germany) or Alexa 568 (Abcam; Thermo Fisher Scientific, Schwerte, Germany), respectively, diluted 1:500 in blocking solution for 2 h at room temperature. After three rinses in PBS, sections were counterstained with 4′,6-diamidino-2-phenylindole (DAPI)-containing solution (1 μg/ml in PBS, Sigma Aldrich) for 3 min at room temperature to visualize nuclei, then rinsed in water and finally mounted in Mowiol (Roth, Karlsruhe, Germany). Control experiments on consecutive tissue sections were performed in which the respective primary antibody was omitted. No immunoreactivity was observed.

Microscopy and imaging

Immunofluorescence was examined and documented with a Zeiss Axiophot microscope (Carl Zeiss MicroImaging, Jena, Germany). Images were captured using a SensiCam CCD camera (PCO Computer Optics, Kelheim, Germany), adjusted for contrast in AxioVision LE Rel. 4.3 (Carl Zeiss MicroImaging, Jena, Germany), and arranged in PowerPoint (Microsoft) or Adobe Photoshop (Adobe Systems, San Jose, CA, USA).

RNA isolation, cDNA synthesis and qPCR

Total RNA was extracted from excised fatty acid-exposed and control strips using the NucleoSpin RNA kit (Macherey-Nagel, Düren, Germany) according to the manufacturer's protocol. To ensure complete DNA removal, a DNase digestion (DNase I, Life Technologies, Carlsbad, CA, USA) step was included. Then, first-strand cDNA was synthesized from 1.5–3 μg total RNA using oligo(dT) primers and SuperScript III Reverse Transcriptase (Invitrogen, Carlsbad, CA, USA). RNA integrity of each sample was confirmed by the amplification of the housekeeping gene encoding the ribosomal protein L8 with intron spanning primers to verify successful DNA removal. Quantitative real-time PCR experiments were performed as previously described (Widmayer et al. 2015). In brief, mRNA levels were assessed using the LightCycler (Roche Diagnostics, Mannheim, Germany). The qPCR mixture (10 μl) consisted of 2× KAPA SYBR Fast qPCR Master Mix (Peqlab Biotechnologie, Erlangen, Germany) and primer sets. For gene amplification, the following primers were used: GPR120 primers: 5′-GTG CCG GGA CTG GTC ATT GTG-3′ and 5′-TTG TTG GGA CAC TCG GAT CTG G-3′ (nt 700–822 from GenBank accession number NM_181748, primers intron spanning, the expected size of PCR products, 123 bp); GPR40 primers: 5′-ATT CCT GGG GTG TGT GTG TGG C-3′ and 5′-AGG CAG TGA TGA CCA AGG GCA G-3′ (AF539809, nt 899–1132, 234 bp), COX-2 primers: 5′-GGG TTG CTG GGG GAA GAA ATG T-3′ and 5′-TCA GGG AGA AGC GTT TGC GGT A-3′ (NM_011198, nt 1449–1568, primers intron spanning, 120 bp); cytokeratin 18 (CK18) primers: 5′-CCG ATA CAA GGC ACA GAT GGA GC-3′ and 5′-GGA GTC CAG GGC ATC GTT GAG A-3′ (BC089022, nt 991–1198, 208 bp), and L8 primers, 5′-GTG CCT ACC ACA AGT ACA AGG C-3′ and 5′-CAG TTT TGG TTC CAC GCA GCC G-3′ (BC043017, nt 548–771, primers intron spanning, 224 bp, 375-bp genomic contamination). Each assay included (in triplicate) 112.5–225 ng of cDNA and a non-template control reaction. The following qPCR protocol was used: 95 °C for 2 min, 95 °C for 15 s, 60 °C (for COX-2 changes) or 62 °C (for FA receptors) for 15 s, 72 °C for 15 s with 45 cycles. Then, a melting curve analysis was included to ensure that only a single, specific amplicon had been produced. Relative amounts of transcripts for GPR120, GPR40 and COX-2 were normalized to the expression of CK18, which remained constant in all samples. Amplification of only one product was additionally confirmed by agarose electrophoresis. Due to almost negligible GPR40 mRNA levels in one sample, no amplification product was detectable. LightCycler Software 3.5 (Roche Diagnostics) results were exported as tab-delimited text files and imported into Microsoft Excel for calculation of the expression ratios using the mean crossing points of target and reference genes from controls and samples.

Western blotting

Total protein was extracted from buffer controls and fatty acid-treated stomach halves and 10–30 μg were loaded onto 10–12.5% SDS-PAGE gels and transferred to nitrocellulose membrane. Immunoblots were blocked with 6% milk powder in PBS containing 0.1% Tween 20 (TBST) for 1 h. Subsequently, the blots were probed with either rabbit anti-ERK1/2 (1:3000), rabbit anti-pERK1/2 (1:500), goat anti-COX-2 (1:100), mouse anti-CK18 (1:200; 61028; Progen Biotechnik, Heidelberg, Germany), or rabbit anti-villin (1:200; GTX109940,

GeneTex, BIOZOL, Eching, Germany) diluted in 5% BSA in TBST overnight at 4 °C. Blots were then incubated with horseradish peroxidase (HRP)–conjugated IgG antisera (goat anti-rabbit IgG and rabbit anti-goat IgG (Sigma Aldrich), goat anti-mouse IgG (Bio-Rad, München, Germany)), all diluted 1:10000 in blocking solution and developed using the Amersham ECL Select kit (Thermo Fisher Scientific). Membranes were scanned using the C-DiGit blot scanner (LI-COR Biotechnology, Bad Homburg, Germany). Bands for ERK1 (44 kDa), pERK1 (44 kDa) and COX-2 (72 kDa) were quantified by relative densitometry after normalization to villin or CK18 using ImageJ (http://rsb.info.nih.gov/ij/).

Cell quantification

For quantitative analyses, only epithelial cells at the most apical layer lining the corpus mucosa were considered. For each animal, 6–8 representative areas were photographically captured at × 40 magnification and cells were manually counted. Positively labeled cells were quantified among DAPI-labeled nuclei of 50 epithelial cells and expressed as percentage or number per 50 epithelial cells. Coexpression of pERK1/2 was determined for each COX-2-immunoreactive brush cell. For COX-2, cell numbers were determined scoring their signal intensities as either weak or moderate to strong. Cells were considered weak when the fluorescent signal was barely above background. Cells that clearly differed in intensity from those with weak signal intensity were rated moderate to strong. Both the percentage and number of positive cells are expressed as a mean ± SD.

Statistical analysis

Transcription rates for GPR40 and GPR120 were normalized to CK18 and determined with the formula $2^{-(\mathrm{Ct\ target}-\mathrm{Ct\ ref})}$. Values are reported as mean ± SEM. For the quantification of relative changes in mRNA expression levels, data were expressed as mean fold differences ± SEM compared with those of controls, with values = 1 representing the baseline level corresponding to no relative difference in expression levels. The formula used to calculate the *n*-fold difference of mRNA expression levels of target genes relative to those of reference genes was as follows: ratio = $(E_{\mathrm{target}})^{\Delta \mathrm{Ct\ target\ (control-sample)}} : (E_{\mathrm{ref}})^{\Delta \mathrm{Ct\ ref\ (control-sample)}}$. Values are expressed as mean ± SEM.

For determination of cell numbers, values are given as mean ± SD. Significant differences were analyzed by the unpaired *t* test with GraphPad Prism (GraphPad Software, www.graphpad.com). Statistical significance was set at $P < 0.05$.

Results

Expression of GPR120 in brush cells of the surface epithelium along the stomach fold

To explore the potential role of GPR120, the receptor for long-chain fatty acids in brush cells, we first performed real-time qPCR and immunohistochemical analyses to investigate the expression, localization and distribution of GPR120-positive cells in the surface epithelium. Real-time qPCR analyses of excised brush cell–containing epithelial strips confirmed a substantial level of expression for *gpr120*, whereas the level of expression for *gpr40*, which also responds to LCFAs, was very low (Fig. 1a). By means of immunohistochemistry and a GPR120 antibody, we obtained numerous labeled cells within the surface epithelium with morphological features typical for brush cells (Fig. 1b). The stained cells had a cylindrical cell body and displayed an either tapering or rounded cell apex. To confirm the identity of the GPR120-positive cells, we assessed the samples for acetylated-α-tubulin (acTub) and for TRPM5, which are considered as markers for structural and transduction components of brush cells (Kaske et al. 2007; Saqui-Salces et al. 2011; Bjerknes et al. 2012). For the experimental studies, we used an acTub antibody and TRPM5-IRES-Cre knockin mice that label TRPM5-expressing cells with τGFP fluorescence (Kusumakshi et al. 2015). As demonstrated in Fig. 1(c–i), several of the GPR120-immunoreactive cells indeed expressed also the marker acTub and TRPM5 confirming that some of the GPR120-positive cells shared brush cell features. Immunostaining for acTub allowed the visualization of the narrow apical microvillar tufts of brush cells (Fig. 1c–f). In order to estimate the proportion of brush cells, which express GPR120, the number of TRPM5-τGFP$^+$ cells in an area comprising 50 surface epithelial cells was counted and the overlap with GPR120 determined. The results indicate that brush cells account for 33.8 ± 5.8% of the epithelial cells; i.e., from 50 epithelial cells, 16.9 ± 2.9 cells were found to be positive for τGFP ($n = 3$). Overall, 69.6 ± 16.1% of the brush cells were found to be costained for GPR120; i.e., from 50 epithelial cells, 12.5 ± 2.9 cells were double-positive for GPR120 and τGFP ($n = 3$) (Fig. 1j). We also observed GPR120 immunoreactivity in a population of epithelial cells that were negative for TRPM5-τGFP, i.e., epithelial cells (Fig. 1k–m).

Expression of ERK1/2 and COX-2 in TRPM5-τGFP$^+$ brush cells

In order to monitor the responses of brush cell to fatty acids, ERK1/2 and COX-2 were considered as suitable indicators.

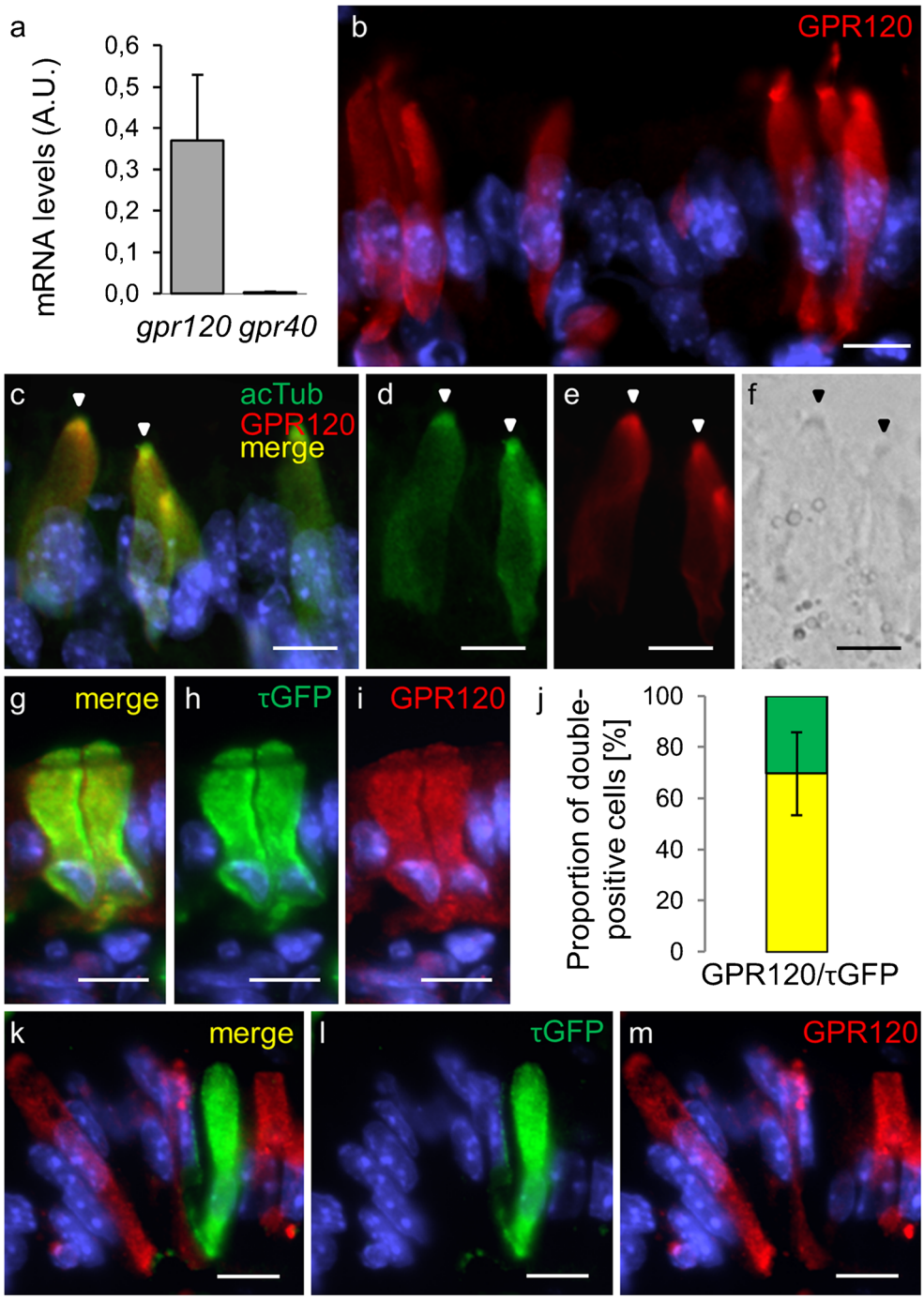

Fig. 1 Visualization and quantification of cells expressing GPR120 in the corpus surface epithelium beneath the limiting ridge of the gastric groove. (**a**) The relative expression levels for *gpr120* and *gpr40* were determined by real-time PCR using cDNA samples from 4 mice. Data are expressed in arbitrary units (a.u.) as mean ± SEM. (**b**) The distribution and clustering pattern of GPR120-labeled cells mimicked that of brush cells. (**c**–**e**) Costaining with acTub (green) revealed that particular GPR120-positive cells (red) display a brush cell–like morphology with distinctive structural characteristics; they have an elongated shape and exhibit prominent apical microtubule bundles. (**f**) DIC of (**d**, **e**) affirms the presence of apical microvilli tufts (indicated by arrow heads). (**g**–**i**) Detection of TRPM5-τGFP (green) confirms that several GPR120-positive cells (red) are brush cells. (**j**) Bar represents the proportion of GPR120 colocalized with TRPM5-τGFP in brush cells (yellow). GPR120-negative TRPM5-τGFP$^+$ cells are indicated in green. (**k**–**m**) In a subset of epithelial cells, no colocalization between GPR120 (red) and TRPM5-τGFP (green) was observed. Scale bars, 10 μm

Therefore, we analyzed whether ERK1/2 and COX-2 are colocalized in TRPM5-τGFP$^+$ brush cells. Immunohistochemical analyses revealed that indeed all TRPM5-τGFP$^+$ brush cells were strongly immunoreactive for ERK1/2 (Fig. 2a–c), while adjacent TRPM5-negative epithelial cells did not show any or only very weak staining. Labeling for COX-2 immunoreactivity was restricted to TRPM5-τGFP$^+$ cells, while adjacent epithelial cells were devoid of any staining. All TRPM5-τGFP$^+$ cells were also positive for COX-2 but exhibited different staining intensities. Brush cells with a prominent COX-2 labeling are depicted in Fig. 2(d–f). Quantification revealed that ERK1/2 and COX-2 were 100% colocalized with TRPM5-τGFP.

Long-chain fatty acid-induced phosphorylation of ERK1/2 in the superficial epithelial lining

The robust expression of ERK1/2 in brush cells encouraged us to employ ERK1/2 phosphorylation to monitor changes in the activity of brush cells upon incubation with fatty acids. For

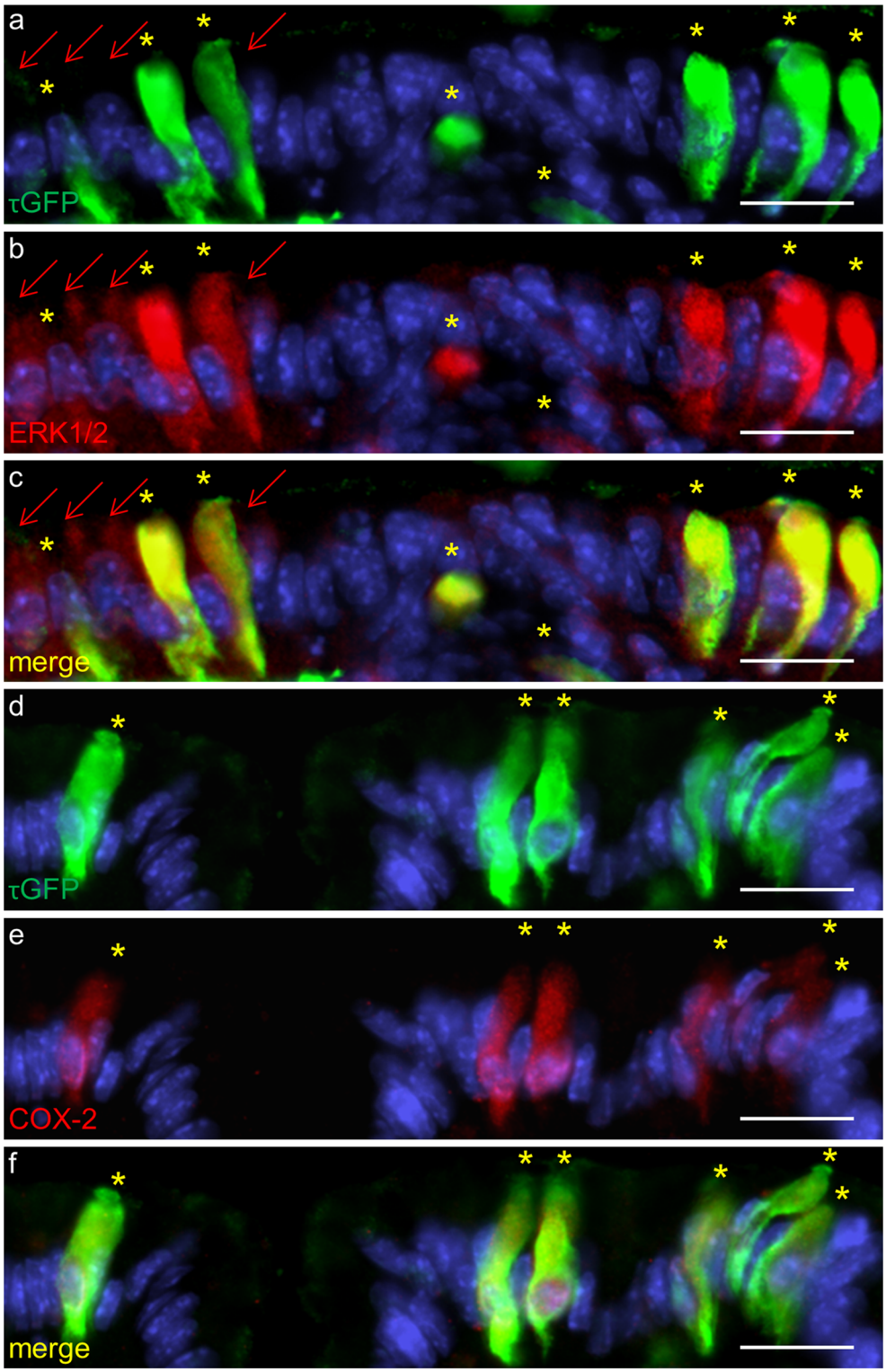

Fig. 2 Double labeling demonstrates a complete overlap between TRPM5-τGFP (**a**) and ERK1/2 (**b**) (indicated by yellow asterisks), as shown in the merged image (**c**). Adjacent cells of the corpus surface epithelium are only weakly stained for ERK1/2 (marked by red arrows). (**d**–**f**) Of the TRPM5-τGFP^{+} brush cells (green), all costained for COX-2 (red). Scale bars, 20 μm

these experiments, the stomach was divided into equal halves and the tissue samples were then incubated either with buffer solution or with buffer solution containing the GPR120 stimuli oleic acid or ALA (10 mM each). After an incubation time of 5 min at 37 °C, a narrow strip comprising the brush cell–containing surface epithelium was isolated from each stomach half. These tissue preparations comprised traces of the uppermost glandular layer of the corpus and remnants of the tissue fold. Strips containing only the tissue fold served as controls. Western blot experiments were performed using antibodies

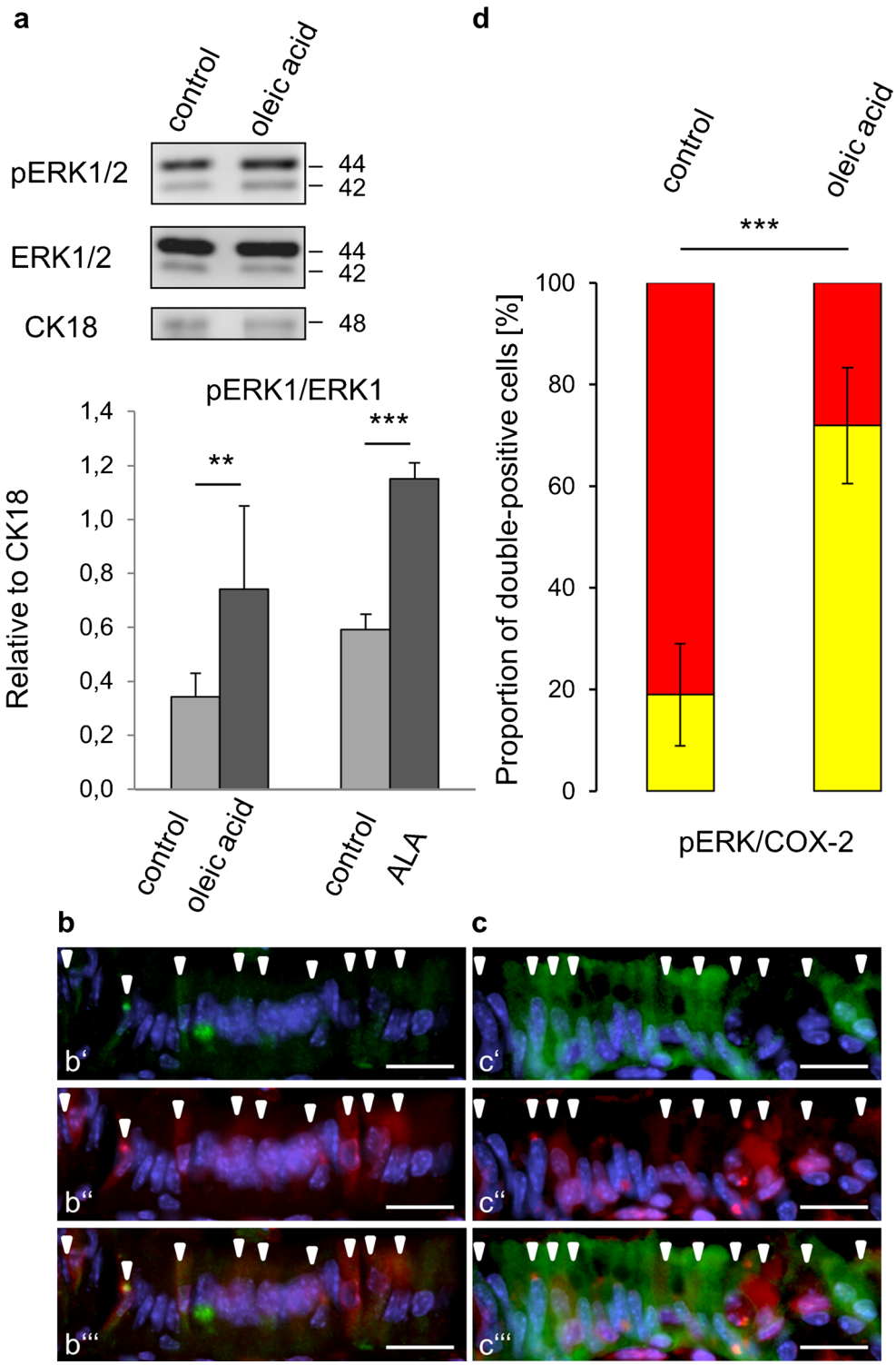

Fig. 3 Effect of LCFAs on ERK1/2 phosphorylation. (**a**) Treatment of stomach tissue with 10 mM oleic acid ($n = 5$) or 10 mM ALA ($n = 3$) for 5 min induced increased ERK1/2 phosphorylation compared to controls treated with buffer solution only. Equal amounts of total protein from excised strips containing surface and uppermost glandular layers were separated by SDS-PAGE and probed with antibodies for pERK1/2 and total ERK1/2. The levels of ERK1/2 protein and phosphorylated ERK1/2 were determined by calculating relative densities of pERK1 and ERK1. The ratio of pERK1 over ERK was normalization to CK18, which was used as the internal loading control for the brush cell preparations. (**b**, **c**) Immunohistochemical analyses revealed that in treated tissue samples (**c**, oleic acid) compared to untreated tissue (**b**, control), pERK1/2 staining (green, **b‘**, **c‘**) was stronger and detectable in more COX-2-positive brush cells (red, **b“**, **c“**) (position indicated by white arrow heads). Note that oleic acid-induced pERK1/2 was also visible in epithelial cells. Merged images (**b“‘**, **c“‘**). **d** Bars represent the proportion of pERK1/2 in COX-2-labeled brush cells upon oleic exposure ($n = 3$). All data are represented as mean ± SD. $^{*}P < 0.05$; $^{**}P < 0.01$; $^{***}P < 0.001$. Scale bar, 20 μm

specific for all ERK1/2 isoforms (ERK1/2) and the phosphorylated ERK1/2 forms (pERK1/2), as well as for CK18 or villin, marker proteins for microvillar cells. The data are depicted in Fig. 3(a) and show that an incubation of tissue samples with 10 mM oleic acid resulted in a significantly higher level of phosphorylated ERK1/2 compared to controls ($P = 0.0047$). Using 10 mM ALA revealed also a significant increase in ERK phosphorylation ($P = 0.0003$) (Fig. 3a), indicating that oleic acid and ALA are suitable stimuli. Application of LCFAs to strips containing only the tissue fold did not lead to changed levels of phosphorylated ERK1/2 (data not shown).

In order to explore whether the higher levels of pERK1/2 induced by LCFAs led to higher pERK1/2 levels in more cells or to a more intense labeling of pERK1/2 cells, immunohistochemical experiments were performed using oleic acid as stimulus. The results depicted in Fig. 3(b)' indicate that pERK1/2 staining under control conditions was only visible in very few cells, whereas numerous pERK1/2-positive cells were visible after oleic acid treatment (Fig. 3c'). The pERK1/2-positive cells seemed to be widely distributed throughout the epithelial layer.

To confirm that activation of ERK1/2 in fact occurred in brush cells, labeling experiments for pERK1/2 and COX-2, as a brush cell marker, were performed. The results indicate that the percentage of colabeled cells was significantly higher; i.e., pERK1/2 could be visualized in more COX-2-positive cells when compared to control conditions (Fig. 3b, c). Quantification revealed that the proportion of COX-2-positive cells with apparent pERK1/2 was increased almost 4-fold ($P < 0.0001$) (Fig. 3d). In addition, phosphorylated ERK was also visible in some adjacent COX-2-negative epithelial cells.

Long-chain fatty acids induce COX-2 expression in brush cells

Based on reports documenting that an activation of the ERK1/2 signaling pathway induced strong expression of COX-2 in other tissues (Rodríguez-Barbero et al. 2006; Xia et al. 2015; Liu et al. 2014), we hypothesized that an increased level of phosphorylated ERK upon exposure to LCFAs might lead to an upregulation of COX-2 expression in brush cells. COX-2 expression is strongly inducible and an elevated level of RNA and protein can already be observed within minutes (Lildal et al. 2017). Moreover, increased levels of COX-2 mRNA and protein seem to coincide with increased cyclooxygenase activity (Bolli et al. 2002; Tamura et al. 2002). Therefore, as a first step, we determined the levels of *cox-2* mRNA in brush cell–containing strips after 5-min exposure to LCFAs by qPCR. It was found that after incubation with oleic acid, the level of *cox-2* mRNA was markedly increased ($P = 0.0014$) (Fig. 4a). Similarly, incubation with ALA also resulted in a marked and significant increase of *cox-2* mRNA levels ($P = 0.0243$) (Fig. 4a). Subsequently, we determined the levels of COX-2 protein. For this purpose, tissue samples were incubated with oleic acid for 10 min and analyzed by Western blots. As shown in Fig. 4(b), the level of COX-2 protein was more than doubled after treatment with oleic acid when compared to that of controls ($P = 0.0177$). In order to determine whether the higher amount of COX-2 protein was due to higher expression levels in brush cells, we visualized COX-2-positive cells using immunohistochemistry. Under control conditions, COX-2 staining was only weak (Fig. 4c, control); however, after oleic acid treatment of the tissue, the intensity of COX-2 labeling was significantly stronger (Fig. 4d, oleic acid). To score the staining intensity, labeled cells were categorized either weak or moderate/strong. Quantification revealed that 1.5 times more brush cells were moderately/strongly labeled after incubation with oleic acid when compared to controls. The data obtained for controls gave a ratio weak versus moderate/strong, 9.7 ± 4.5 versus 6.5 ± 3.2, whereas the data after oleic acid treatment resulted in a ratio weak versus moderate/strong, 7.9 ± 5.0 versus 9.6 ± 4.7 (weak: $P = 0.0397$, moderate/strong: $P < 0.0001$) (Fig. 4e) per 50 epithelial cells. It is conceivable that the more strongly labeled brush cells (55%) may represent the subpopulation that expresses the GPR120 receptor.

Discussion

Brush cells at the limiting ridge of the stomach express the receptor GPR120 (Janssen et al. 2012; Widmayer et al. 2015), which recognizes long-chain fatty acids (> C12) (Hirasawa et al. 2005; Tanaka et al. 2008). The presence of the LCFA receptor GPR120 in a large population of brush cells implies that these cells are responsive to fatty acids, such as oleic acid and α-linolenic acid. This notion was confirmed by monitoring the phosphorylation of ERK1/2 in the superficial epithelial lining of the corpus. Our results indicate that oleic acid evokes phosphorylation of ERK1/2 in about 70% of the brush cells, comparable to the proportion of brush cells that express GPR120. Activation of the ERK1/2 pathway is involved in regulating a large variety of molecular processes and, depending on the cell type and the cellular environment, can affect many different aspects of cell physiology (for review, see Shaul and Seger 2007). Thus, it can be assumed that LCFAs elicit distinct physiological responses in brush cells at the limiting ridge. Along the stomach fold, brush cells form a band of clustered cells intermingled by epithelial cells (Luciano and Reale 1992) and oleic acid-induced ERK1/2 phosphorylation was also seen in epithelial cells adjacent to brush cells. Expression of GPR120 was not strictly specific for brush cells but also seen in some epithelial cells; thus, it is possible that in those cells, ERK1/2 phosphorylation induced by oleic acid is mediated via receptor activation. However, pERK1/2 was often visible in epithelial cells directly adjacent to brush cells. Hence, LCFA-induced phosphorylation of ERK1/2 in neighboring epithelial cells may be due to paracrine signaling originating from the activated brush cells. Interestingly, it has recently been reported that cell-cell spinules exist in the brush cells of the intestine, which might allow an intense intercellular communication (Hoover et al. 2017). However, there is no evidence for such structures in gastric brush cells.

It has been proposed that brush cells at the limiting ridge operate as sensory cells and provide information via local chemical messengers to neighboring cells or nerve fibers (Eberle et al. 2013a, b). Since brush cells appear to lack

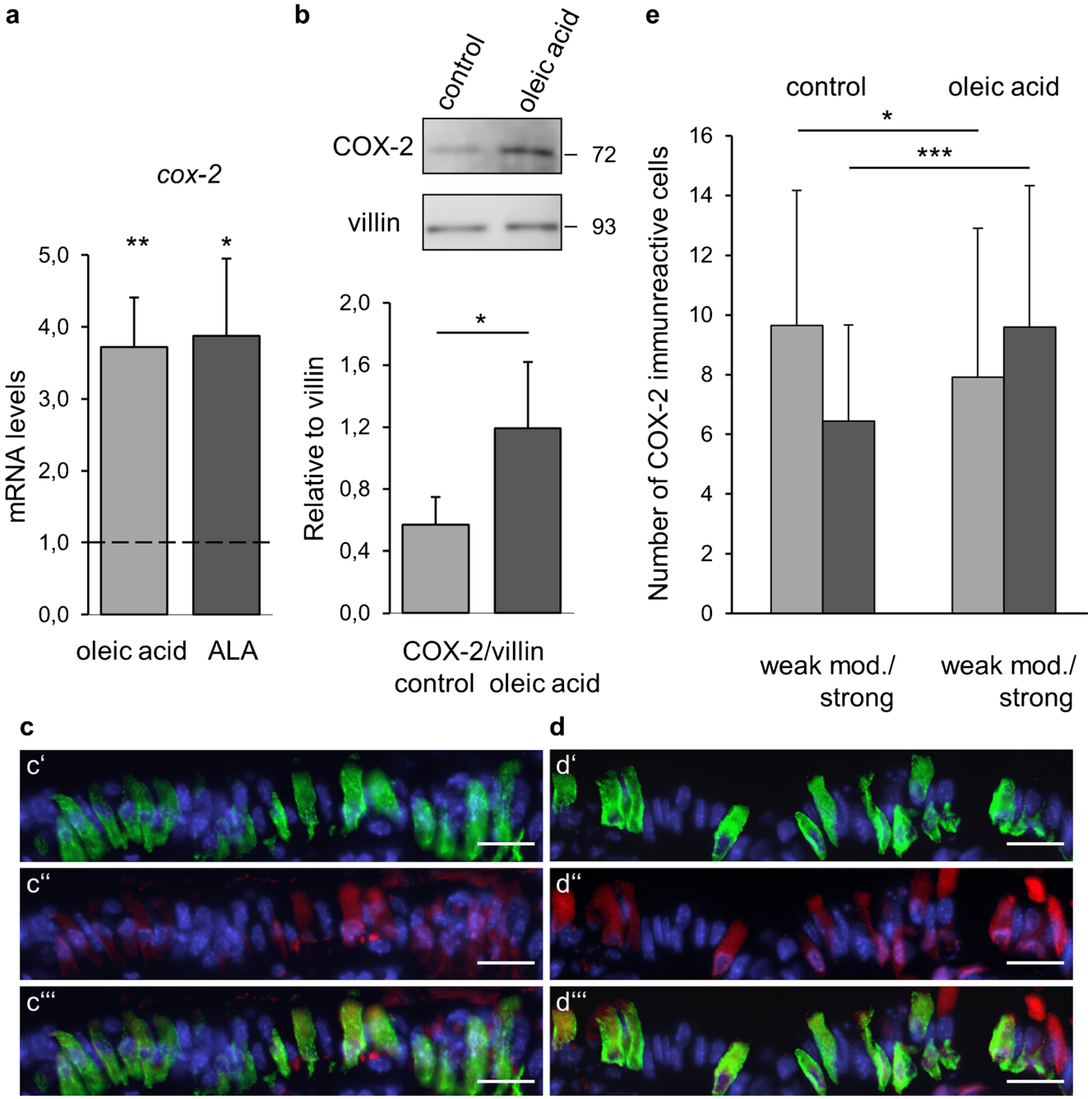

Fig. 4 LCFAs induce enhanced COX-2 expression in brush cells. (**a**) The results of qPCR analyses indicate that the level of *cox-2* mRNA in brush cell–containing strips was markedly higher after a 5-min treatment with either 10 mM oleic acid ($n = 3$) or 10 mM ALA ($n = 4$) than that of controls denoted by the dashed line. Data are expressed as mean fold differences ± SEM, with values = 1 representing the baseline level of controls that corresponds to no relative changes. (**b**) 10-min treatment of stomach tissue with 10 mM oleic acid caused enhanced protein levels of COX-2. The level of COX-2 protein was determined to normalized villin, which was used as internal loading control ($n = 5$). (**c**, **d**) Comparison of COX-2 (red, **c“**, **d“**) and TRPM5 (green, **c‘**, **d‘**) labeling in brush cells upon a treatment with oleic acid. An increased number of stronger COX-2-labeled brush cells were observed upon oleic acid exposure (**d**, oleic acid) compared to untreated tissue (**c**, control). Merged images (**c“‘**, **d“‘**). (**e**) Classification of COX-2-labeled cells into weak versus moderate/strong resulted in a shift in the ratio of more moderate/strong signals in treated oleic acid ($n = 5$). Data are represented as mean ± SD. $^{*}P < 0.05$; $^{**}P < 0.01$; $^{***}P < 0.001$. Scale bar, 20 μm

secretory granules (Kokrashvili et al. 2009), it seems conceivable that signaling molecules that are de novo synthesized are used in response to external stimuli. Prostaglandins are potential candidate molecules since the rate-limiting enzymes COX-1 and COX-2 are specifically expressed in brush cells (Bezençon et al. 2008; Eberle et al. 2013b, Schütz et al. 2015).

Consistent with this, we found that application of LCFAs induced an increased level of COX-2 in the tissue and enhanced immunohistochemical signals for COX-2 were observed in more than half of the brush cells. Since the ERK1/2 signaling pathway can regulate COX-2 at the level of both transcription and translation (Tung et al. 2009; McElroy et al. 2012; Xia et al. 2015), it is conceivable that ERK1/2 phosphorylation induced by LCFAs may be linked to the upregulation of COX-2 expression in brush cells. An induced expression of the non-constitutive COX-2 is supposed to result in an enhanced prostaglandin formation (Liu et al. 2014).

Functional implications of LCFA-induced prostaglandin production in brush cells at the fundus/corpus border of the stomach are not immediately obvious. However, prostaglandin-mediated regulation of local secretory and gastro-protective processes has been documented (Araki et al. 2000; Flemström 1986; Brzozowski et al. 2005). Thus, it is conceivable that prostaglandins may cause a release of gastric lipase from chief cells (Liao et al. 1983), an increased generation of bicarbonate (Takeuchi et al. 1997), or an inhibition of gastric acid secretion (Robert 1979). Another possible role of prostaglandins might be the activation of superficial cells of the corpus mucosa triggering the production of mucins and/or trefoil peptides, which are important for mucosal protection (Mao et al. 2012). Consequently, certain dietary fatty acids may be important for promoting the synthesis of the biologically active messengers, which in turn might help to fortify the mucosal barrier (Hollander and Tarnawski 1991).

In conclusion, based on our results, we propose that long-chain fatty acids, such as oleic acid and α-linolenic acid, elicit an activation of the ERK1/2 pathway via GPR120, which in turn induces the expression of COX-2 and ultimately leads to the generation of prostaglandins, which may act as paracrine messengers. Consequently, sensing of long-chain fatty acids may be relevant for a local regulation of gastric processes, such as secretion or gastro-protection.

Acknowledgements We thank Kerstin Bach for her excellent technical assistance and Marilena Lieber for her skillful experimental support and advice. We would like to express our gratitude to T. Gudermann and V. Chubanov for generously providing the TRPM5 antibody.

Funding information This work was supported by the Deutsche Forschungsgemeinschaft, BR 712/25-1, BO 1743/3 and SFB/TR152.

Compliance with ethical standards The authors declare that the study complies with accepted principles of ethical and professional conduct.

Conflict of interest The authors declare that they have no conflict of interest.

Ethical approval All applicable international (Council Directive 2010/63EU of the European Parliament and the Council of 22 September 2010 on the protection of animals used for scientific purposes), national (work was approved by the Committee on the Ethics of Animal Experiments at the Regierungspräsidium Stuttgart V318/14 PHY) and institutional guidelines for the care and use of animals were followed. All procedures performed in studies involving animals were in accordance with the ethical standards of the institution or practice at which the studies were conducted (University of Hohenheim Animal Welfare Officer T125/14 PHY, T126/14 PHY).

Publisher's Note Springer Nature remains neutral with regard to jurisdictional claims in published maps and institutional affiliations.

References

Araki H, Ukawa H, Sugawa Y, Yagi K, Suzuki K, Takeuchi K (2000) The roles of prostaglandin E receptor subtypes in the cytoprotective action of prostaglandin E2 in rat stomach. Aliment Pharmacol Ther 1: 116–124

Bezençon C, Fürholz A, Raymond F, Mansourian R, Métairon S, Le Coutre J, Damak S (2008) Murine intestinal cells expressing Trpm5 are mostly brush cells and express markers of neuronal and inflammatory cells. J Comp Neurol 509:514–525. https://doi.org/10.1002/cne.21768

Bjerknes M, Khandanpour C, Möröy T, Fujiyama T, Hoshino M, Klisch TJ, Ding Q, Gan L, Wang J, Martín MG, Cheng H (2011) Origin of the brush cell lineage in the mouse intestinal epithelium. Dev Biol 2012 362:194–218. https://doi.org/10.1016/j.ydbio.2011.12.009

Bolli R, Shinmura K, Tang XL, Kodani E, Xuan YT, Guo Y, Dawn B (2002) Discovery of a new function of cyclooxygenase (COX)-2: COX-2 is a cardioprotective protein that alleviates ischemia/reperfusion injury and mediates the late phase of preconditioning. Cardiovasc Res 55:506–519

Brown MD, Sacks DB (2009) Protein scaffolds in MAP kinase signalling. Cell Signal 21:462–469. https://doi.org/10.1016/j.cellsig.2008.11.013

Brzozowski T, Konturek PC, Konturek SJ, Brzozowska I, Pawlik T (2005) Role of prostaglandins in gastroprotection and gastric adaptation. J Physiol Pharmacol 5:33–55

Eberle JA, Richter P, Widmayer P, Chubanov V, Gudermann T, Breer H (2013a) Band-like arrangement of taste-like sensory cells at the gastric groove: evidence for paracrine communication. Front Physiol 4: 58. https://doi.org/10.3389/fphys.2013.00058 eCollection 2013

Eberle JA, Müller-Roth KL, Widmayer P, Chubanov V, Gudermann T, Breer H (2013b) Putative interaction of brush cells with bicarbonate secreting cells in the proximal corpus mucosa. Front Physiol 4:182. https://doi.org/10.3389/fphys.2013.00182 eCollection 2013

Flemström G (1986) Gastroduodenal mucosal secretion of bicarbonate and mucus. Physiologic control and stimulation by prostaglandins. Am J Med 81:18–22

Frantz JD, Betton G, Cartwright ME, Crissman JW, Macklin AW, Maronpot RR (1991) Proliferative lesions of the non-glandular and glandular stomach in rats, GI-3. In: Guides for Toxicologic Pathology. STP/ARP/AFIP, Washington, DC, p 1–20

Hass N, Schwarzenbacher K, Breer H (2007) A cluster of gustducin-expressing cells in the mouse stomach associated with two distinct populations of enteroendocrine cells. Histochem Cell Biol 128:457–471. https://doi.org/10.1007/s00418-007-0325-3

Hirasawa A, Tsumaya K, Awaji T, Katsuma S, Adachi T, Yamada M, Sugimoto Y, Miyazaki S, Tsujimoto G (2005) Free fatty acids regulate gut incretin glucagon-like peptide-1 secretion through GPR120. Nat Med 11:90–94

Höfer D, Püschel B, Drenckhahn D (1996) Taste receptor-like cells in the rat gut identified by expression of alpha-gustducin. Proc Natl Acad Sci U S A 93:6631–6634. https://doi.org/10.1073/pnas.93.13.6631

Hollander D, Tarnawski A (1991) Is there a role for dietary essential fatty acids in gastroduodenal mucosal protection? J Clin Gastroenterol 13:72–74

Hoover B, Baena V, Kaelberer MM, Getaneh F, Chinchilla S, Bohórquez DV (2017) The intestinal tuft cell nanostructure in 3D. Sci Rep 7: 1652. https://doi.org/10.1038/s41598-017-01520-x

Janssen S, Laermans J, Iwakura H, Tack J, Depoortere I (2012) Sensing of fatty acids for octanoylation of ghrelin involves a gustatory G-protein. PLoSOne 7:e40168. https://doi.org/10.1371/journal.pone.0040168

Kaske S, Krasteva G, König P, Kummer W, Hofmann T, Gudermann T, Chubanov V (2007) TRPM5, a taste-signaling transient receptor potential ion-channel, is a ubiquitous signaling component in chemosensory cells. BMC Neurosci 8:49. https://doi.org/10.1186/1471-2202-8-49

Kokrashvili Z, Rodriguez D, Yevshayeva V, Zhou H, Margolskee RF, Mosinger B (2009) Release of endogenous opioids from duodenal enteroendocrine cells requires Trpm5. Gastroenterology 137:598–606, 606.e1-2. https://doi.org/10.1053/j.gastro.2009.02.070

Kugler P, Höfer D, Mayer B, Drenckhahn D (1994) Nitric oxide synthase and NADP-linked glucose-6-phosphate dehydrogenase are colocalized in brush cells of rat stomach and pancreas. J Histochem Cytochem 42:1317–1321

Kusumakshi S, Voigt A, Hübner S, Hermans-Borgmeyer I, Ortalli A, Pyrski M, Dörr J, Zufall F, Flockerzi V, Meyerhof W, Montmayeur JP, Boehm U (2015) A binary genetic approach to characterize TRPM5 cells in mice. Chem Senses 40:413–425. https://doi.org/10.1093/chemse/bjv023

Liao TH, Hamosh P, Hamosh M (1983) Gastriclipolysis in the developing rat. Ontogeny of the lipases active in the stomach. Biochim Biophys Acta 754:1–9

Lildal SK, Nørregaard R, Andreassen KH, Christiansen FE, Jung H, Pedersen MR, Osther PJ (2017) Ureteral access sheath influence on the ureteral wall evaluated by cyclooxygenase-2 and tumor necrosis factor-α in a porcine model. J Endourol 31:307–313. https://doi.org/10.1089/end.2016.0773

Liu Y, Chen LY, Sokolowska M, Eberlein M, Alsaaty S, Martinez-Anton A, Logun C, Qi HY, Shelhamer JH (2014) The fish oil ingredient, docosahexaenoic acid, activates cytosolic phospholipase A_2 via GPR120 receptor to produce prostaglandin E_2 and plays an anti-inflammatory role in macrophages. Immunology 143:81–95. https://doi.org/10.1111/imm.12296

Luciano L, Reale E (1992) The "limiting ridge" of the rat stomach. Arch Histol Cytol 55:131–138. https://doi.org/10.1679/aohc.55.Suppl_131

Mao W, Chen J, Peng TL, Yin XF, Chen LZ, Chen MH (2012) Role of trefoil factor 1 in gastric cancer and relationship between trefoil factor 1 and gastrokine 1. Oncol Rep 28:1257–1262. https://doi.org/10.3892/or.2012.1939

Matsukura N, Asano G (1997) Anatomy, histology, ultrastructure, stomach, rat. In: Jones TC, Popp JA, Mohr U (eds) Monographs on Pathology of Laboratory Animals. Digestive system, 2nd edn. Springer, Berlin, pp 343–350

McElroy SJ, Hobbs S, Kallen M, Tejera N, Rosen MJ, Grishin A, Matta P, Schneider C, Upperman J, Ford H, Polk DB, Weitkamp JH (2012) Transactivation of EGFR by LPS induces COX-2 expression in enterocytes. PLoS One 7:e38373. https://doi.org/10.1371/journal.pone.0038373

Robert A (1979) Cytoprotection by prostaglandins. Gastroenterology 77: 761–767

Rodríguez-Barbero A, Dorado F, Velasco S, Pandiella A, Banas B, López-Novoa JM (2006) TGF-beta1 induces COX-2 expression and PGE2 synthesis through MAPK and PI3K pathways in human mesangial cells. Kidney Int 70:901–909

Saqui-Salces M, Keeley TM, Grosse AS, Qiao XT, El-Zaatari M, Gumucio DL, Samuelson LC, Merchant JL (2011) Gastric tuft cells express DCLK1 and are expanded in hyperplasia. Histochem Cell Biol 136:191–204. https://doi.org/10.1007/s00418-011-0831-1

Schütz B, Jurastow I, Bader S, Ringer C, von Engelhardt J, Chubanov V, Gudermann T, Diener M, Kummer W, Krasteva-Christ G, Weihe E (2015) Chemical coding and chemosensory properties of cholinergic brush cells in the mouse gastrointestinal and biliary tract. Front Physiol 6:87. https://doi.org/10.3389/fphys.2015.00087 eCollection2015

Shaul YD, Seger R (2007) The MEK/ERK cascade: from signaling specificity to diverse functions. Biochim Biophys Acta 1773:1213–1226

Symonds EL, Peiris M, Page AJ, Chia B, Dogra H, Masding A, Galanakis V, Atiba M, Bulmer D, Young RL, Blackshaw LA (2015) Mechanisms of activation of mouse and human enteroendocrine cells by nutrients. Gut 64:618–826. https://doi.org/10.1136/gutjnl-2014-306834

Takeuchi K, Yagi K, Kato S, Ukawa H (1997) Roles of prostaglandin E-receptor subtypes in gastric and duodenal bicarbonate secretion in rats. Gastroenterology 113:1553–1559

Tamura M, Sebastian S, Yang S, Gurates B, Fang Z, Bulun SE (2002) Interleukin-1beta elevates cyclooxygenase-2 protein level and enzyme activity via increasing its mRNA stability in human endometrial stromal cells: an effect mediated by extracellularly regulated kinases 1 and 2. J Clin Endocrinol Metab 87:3263–3273

Tanaka T, Yano T, Adachi T, Koshimizu TA, Hirasawa A, Tsujimoto G (2008) Cloning and characterization of the rat free fatty acid receptor GPR120: in vivo effect of the natural ligand on GLP-1 secretion and proliferation of pancreatic beta cells. Naunyn Schmiedeberg's Arch Pharmacol 377:515–522. https://doi.org/10.1007/s00210-007-0250-y

Tung WH, Hsieh HL, Yang CM (2009) Enterovirus71 induces COX-2 expression via MAPKs, NF-kappaB, and AP-1 in SK-N-SH cells: role of PGE(2) in viral replication. Cell Signal 22:234–246. https://doi.org/10.1016/j.cellsig.2009.09.018

van der Heijden M, Zimberlin CD, Nicholson AM, Colak S, Kemp R, Meijer SL, Medema JP, Greten FR, Jansen M, Winton DJ, Vermeulen L (2016) Bcl-2 is a critical mediator of intestinal transformation. Nat Commun 7:10916. https://doi.org/10.1038/ncomms10916

Widmayer P, Goldschmid H, Henkel H, Küper M, Königsrainer A, Breer H (2015) High fat feeding affects the number of GPR120 cells and enteroendocrine cells in the mouse stomach. Front Physiol 6:53. https://doi.org/10.3389/fphys.2015.00053 eCollection 2015

Xia Q, Hu Q, Wang H, Yang H, Gao F, Ren H, Chen D, Fu C, Zheng L, Zhen X, Ying Z, Wang G (2015) Induction of COX-2-PGE2 synthesis by activation of the MAPK/ERK pathway contributes to neuronal death triggered by TDP-43-depleted microglia. Cell Death Dis 6:e1702. https://doi.org/10.1038/cddis.2015.69